Felicitas Kolbe, Simon Krause, Volodymyr Bon, Irena Senkovska, Stefan Kaskel, Eike Brunner

High-Pressure in Situ ^{129}Xe NMR Spectroscopy: Insights into Switching Mechanisms of Flexible Metal–Organic Frameworks Isoreticular to DUT-49

Erstveröffentlichung in / First published in:

Chemistry of materials. 2019, 31 (16), S. 6193-6201. American Chemical Society. ISSN 1520-5002.

DOI: http://dx.doi.org/10.1021/acs.chemmater.9b02003

High Pressure *In Situ* ^{129}Xe NMR Spectroscopy: Insights into Switching Mechanisms of Flexible Metal-Organic Frameworks Isoreticular to DUT-49

Felicitas Kolbe,[1] Simon Krause,[2] Volodymyr Bon,[2] Irena Senkovska,[2] Stefan Kaskel,[2] Eike Brunner[1,*]

[†] Faculty of Chemistry and Food Chemistry, Chair of Bioanalytical Chemistry, TU Dresden, D-01062 Dresden, Germany

[‡] Faculty of Chemistry and Food Chemistry, Chair of Inorganic Chemistry I, TU Dresden, D-01062 Dresden, Germany

Supporting Information Placeholder

ABSTRACT: Flexible metal-organic frameworks (MOFs) are capable of changing their crystal structure as a function of external stimuli such as pressure, temperature, and type of adsorbed guest species. DUT-49 is the first MOF exhibiting structural transitions accompanied by the counterintuitive phenomenon of negative gas adsorption (NGA). Here, we present high pressure *in situ* ^{129}Xe NMR spectroscopic studies of a novel isoreticular MOF family based on DUT-49. These porous materials differ only in the length of their organic linkers causing changes in pore size and elasticity. The series encompasses both, purely microporous materials as well as materials with both, micropores and small mesopores. The chemical shift of adsorbed xenon depends on xenon-wall interactions and thus, on the pore size of the material. The xenon adsorption behavior of the different MOFs can be observed over the whole range of relative pressure. Chemical shift adsorption/desorption isotherms closely resembling the conventional, uptake-measurement based isotherms were obtained at 237 K where all materials are rigid. The comparable chemical environment for adsorbed xenon in these isoreticular MOFs allows establishing a correlation between the chemical shift at a relative pressure of $p/p_0 = 1.0$ and the mean pore diameter. Furthermore, the xenon adsorption behavior of the MOFs is studied also at 200 K. Here, structural flexibility is found for DUT-50, a material with an even longer linker than the previously known DUT-49. Its structural transitions are monitored by ^{129}Xe NMR spectroscopy. This compound is the second known MOF showing the phenomenon of negative gas adsorption. Further increase in the linker length results in DUT-151, a material with interpenetrated network topology. *In situ* ^{129}Xe NMR spectroscopy proves that this material exhibits another type of flexibility compared to DUT-49 and DUT-50. Further surprising observations are made for DUT-46. Volumetric xenon adsorption measurements show that this non-flexible microporous material does not exhibit any hysteresis. In contrast, *in situ* ^{129}Xe NMR spectroscopically detected xenon chemical shift isotherms exhibit a hysteresis even after longer equilibration times than in the volumetric experiments. This indicates kinetically hindered re-distribution processes and long-lived metastable states of adsorbed xenon within the MOF persisting at the time scale of hours or longer.

INTRODUCTION

Metal-organic frameworks (MOFs) are highly porous hybrid materials based on inorganic secondary building units (SBUs) which are connected by organic linkers.[1,2] Their properties can be tuned by varying the length and functionalization of the organic linkers.[3,4] Thus, MOFs became a research field of increasing interest.[1] Low densities (down to 0,124 g/cm^3)[5] and high surface areas (up to 7839 m^2/g)[6] render the materials suitable for various applications. They are explored with respect to gas and energy storage, gas separation, catalysis, sensing, and as drug delivery systems in biomedicine.[1,2,4,7–9] Before applying MOFs in gas storage and separation, it is especially important to characterize the adsorption processes inside the pore system. Flexible MOFs are a peculiar subgroup of MOFs with unique properties. They undergo structural transitions induced by external stimuli such as temperature, pressure, and presence of guest molecules. Famous examples are MIL-53, SNU-9, DUT-8 and many others.[10–12]

The recently discovered material DUT-49 (*Dresden University of Technology No.*49) is the first flexible MOF showing the surprising phenomenon of negative gas adsorption (NGA).[13] Adsorbed gases such as methane or xenon are partly released from the structure at increasing pressure during the structural transition from the open-pore (***op***) into the contracted-pore (***cp***) state. Inspired by this observation, an isoreticular series was synthesized which differs from DUT-49 only in the length of the linker molecule (cf. Figure 1). The xenon adsorption behavior of this isoreticular series is investigated within the present work using high pressure *in situ* ^{129}Xe NMR spectroscopy.

NMR-spectroscopy offers two general approaches to study porous materials like MOFs: On one hand, it is pos-

sible to investigate the structure and dynamics of the material itself by observing NMR-active nuclei in the corresponding compound, such as ^{13}C or ^{1}H.[14–16] On the other hand, it is possible to load the materials with NMR-active probe molecules or atoms, thus, exploiting host-guest interactions. Gases like CO_2 or Xe are often applied as probe.[17–25]

Due to its large electron cloud, the NMR chemical shift of xenon exhibits a high sensitivity. Therefore, ^{129}Xe (I = 1/2) with a natural abundance of 26.4 % is a well-suited probe to study surfaces.[26-29] The chemical shift of adsorbed xenon in porous materials like zeolites[28–30] or MOFs[31] can be written as:

$$\delta = \delta_s + \delta_{Xe-Xe}(\rho_{Xe}, T) \quad [1]$$

The first term, δ_s, reflects all contributions due to interactions between xenon atoms and the different surface sites of the pore system. The second term, $\delta_{Xe\text{-}Xe}$, describes the interactions between adsorbed xenon atoms and depends on the density of xenon ρ_{Xe} and the temperature.[26-28]

Since adsorbed xenon is mobile and can undergo rapid exchange and diffusion processes inside the pore system, two fundamentally different cases must be distinguished: (i) Compounds with pores large enough to adsorb xenon but rather small interconnecting windows/channels preventing fast exchange processes between neighboring pores. Note that the diameter of xenon amounts to ca. 4.4 Å. (ii) Compounds with pores interconnected by sufficiently large windows/channels allowing rapid xenon diffusion between different pores. A striking example for case (i) are the zeolites Na-A and Ag-A.[32–35] Xenon clusters of different size are then formed inside the different pores - without fast exchange between neighboring pores. This results in an ensemble of lines of different chemical shift caused by the influence of Xe-Xe interactions which depend on the cluster size (cf. eq. [1]). Recently, this behavior was also observed for a special MOF denoted as MFU-4 with remarkably small pore apertures of only 2.4 Å diameter.[36] Quite often, however, case (ii) is observed. Rapid diffusion of xenon atoms through the pore system then results in a single line with a chemical shift representing the weighted average along the trajectory of xenon. Note that the shape of this line is not necessarily symmetric. For materials with anisotropic pore systems, the line shape of adsorbed xenon can be anisotropic as demonstrated previously.[37–42] Note that the line shape is not only depending on intracrystalline exchange and diffusion, but also on intercrystalline exchange processes.[41] Thus, ^{129}Xe NMR spectroscopy provides information about adsorption processes as well as xenon dynamics in various porous materials.[26–51]

Here, high pressure *in situ* ^{129}Xe NMR spectroscopy is used to investigate host-guest interactions under controlled thermodynamic conditions. The homebuilt high pressure apparatus[51] allows *in situ* experiments at variable pressures up to saturation and at temperatures down to 195 K. In addition to the previously studied DUT-49, a novel series of MOFs including the materials DUT-48, DUT-46, and DUT-50 was studied. These MOFs are built from copper paddle-wheels and carbazole-3,6-dicarboxylate forming metal-organic polyhedrons (MOPs). These MOPs constitute small cuboctahedral pores. Connecting the MOPs with tetratopic, organic linkers results in a framework which consists of three different types of pores. In addition to the cuboctahedral pores, tetrahedral and octahedral cavities are formed (cf. Figure 1, a-d).[52] The length of the organic linkers is varied within the MOF family (Figure 1, e-h) resulting in MOFs of different pore size and inner surface area (Table 1). The functionalization of the organic linkers as well as the MOP structure remains unchanged. DUT-49 shows an extremely high methane storage capacity.[52] Comparative investigation of the new isoreticular series thus allows to study differences in the adsorption behavior which are purely introduced by the different linkers. Furthermore, it is speculated that the pore size may correlate with the chemical shift of adsorbed xenon due to the similarity in surface chemistry provided by this special MOF series.

Table 1. Calculated pore sizes of DUT-48, DUT-46, DUT-49, and DUT-50.

	octahedral-pore / Å	tetrahedral pore / Å	cuboctahedral pore / Å
DUT-48	18.7	14.8	10.7
DUT-46	21.8	15.0	10.7
DUT-49	24.8	17.6	10.5
DUT-50	30.7	21.0	10.7

EXPERIMENTAL SECTION

The dried MOFs were stored under an inert, dry atmosphere. For the experiments, the samples were transferred into a single crystal sapphire tube and activated overnight (100 °C, 10^{-5} mbar). The high pressure *in situ* experiments were carried out using a homebuilt apparatus.[51] A defined xenon pressure can be adjusted. All experiments were carried out on an Avance 300 NMR-spectrometer (Bruker, Germany) equipped with a HR probe. The NMR spectra were recorded at a resonance frequency of 83.04 MHz for ^{129}Xe using a pulse length of 11 µs and relaxation delays of 15 s. A BIOSPIN SA BCU-Xtreme unit (Bruker, Germany) was used for sample cooling. Measurements were carried out at two different temperatures, 237 K and 200 K. To obtain adsorption/desorption isotherms the chemical shift of adsorbed xenon was observed over the whole range of pressure up to a relative pressure $p/p_0 = 1$. Equilibration times of 15 min after pressure changes and 30 min after temperature changes were used. The temperature calibration was

carried out using the ^{1}H signal of methanol.[53,54] As a second method of temperature calibration, the condensation pressure of xenon was used to determine the corresponding temperature from the phase diagram. The chemical shift is referenced relative to xenon gas extrapolated to zero pressure.

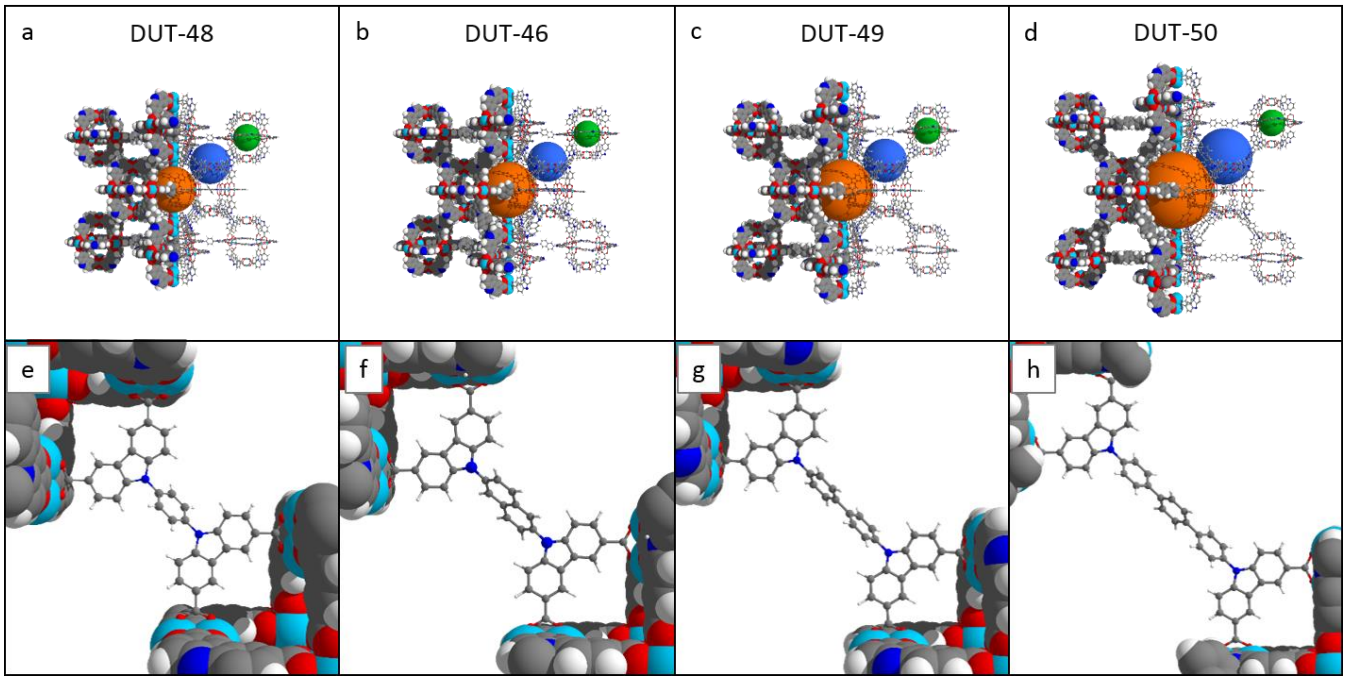

Figure 1. Structure of investigated metal-organic frameworks and their corresponding organic linkers a) DUT-48, b) DUT-46, c) DUT-49 and d) DUT-50. Color code: Cu – turquoise, O – red, C – grey, N – blue, H – white, cuboctahedral pore – green, tetrahedral pore – blue, octahedral pore – orange.

RESULTS AND DISCUSSION

The flexibility of DUT-49, i.e., its phase transformations, do not only depend on the type of adsorbed gas, but also on the temperature. In the case of xenon adsorption, it behaves like a rigid MOF at 237 K, but is flexible at 200 K. Therefore, isothermal *in situ* ^{129}Xe NMR experiments were performed at these two temperatures for the isoreticular series studied here as well.

Experiments at 237 K. ^{129}Xe NMR spectra were recorded at various pressures covering the entire relative pressure range at constant temperature. Such measurements result in chemical shift adsorption/desorption isotherms. Figure 2 compares the chemical shift isotherms for the purely microporous material DUT-48, as well as DUT-46 and DUT-50, which exhibit micropores and small mesopores (cf. Table 1). This comparison reveals striking differences for the three chemical shift isotherms. First of all, the shape of the chemical shift isotherm of DUT-48 resembles a reversible Type I(b) isotherm.[55] This observation can be explained by the fact that the ^{129}Xe NMR chemical shift is correlated with the amount of xenon adsorbed in the pores as predicted by the second term of eq. [1]. This correlation is the reason for the similarity between conventional adsorption/desorption isotherms obtained by uptake measurements (in mass or volume units) and the chemical shift isotherms presented here. Similar correlations were already observed by our group[56] for the microporous MOFs UiO-66 and UiO-67 (*Universitetet i Oslo*).[57] After a steep, almost linear increase at low relative pressure, the isotherm starts to level off for $p/p_0 > 0.4$. The initial regime with its linear behavior is well known for other microporous materials such as zeolites.[28,55] In contrast to DUT-48, the isotherm of DUT-50 exhibits the characteristic S-shape (Type IV) expected for mesoporous materials.[55] At lower relative pressures, the present micropores are preferentially filled and only a monolayer of xenon atoms is adsorbed in the mesopores. With increasing relative pressure, multilayer adsorption occurs inside the mesopores which finally results in capillary condensation. Therefore, a plateau is finally observed indicating that the maximum possible density is reached as also observed for the microporous DUT-48. However, xenon desorption during pressure release shows a hysteresis compared to the adsorption branch for the mesoporous DUT-50; a characteristic behavior for capillary condensation inside mesopores. The isotherm of DUT-46 is located between the two cases described above. The chemical shift isotherm shows a Type I(b) shape. However, the chemical shift increase is slower than for DUT-48 and the plateau is finally reached at higher relative pressure. This is due to the larger pores of the material. Nevertheless, the obtained isotherm is reversible.

It is, furthermore, interesting to note that the chemical shift of the adsorbed xenon exceeds the chemical shift of liquid xenon at the given temperature and high relative pressure. The chemical shift of ^{129}Xe at $p/p_0 = 1$ can be determined very precisely by extrapolation of the chemical shift since the slope of the isotherm decreases and is almost zero at relative pressures close to one. It can be concluded from this observation in combination with eq. [1] that the xenon density inside the pores only slightly changes at sufficiently high relative pressures, i.e., that the pore system is filled at p/p_0 close to 1. A chemical shift difference $\Delta\delta$ is observed between the chemical shift $\bar{\delta}$ resulting from the extrapolation of δ to $p/p_0 = 1$ and the chemical shift δ_B of bulk liquid xenon of ca. 197 ppm at the given measurement temperature. This difference arises due to the fact that a certain fraction of xenon atoms is in direct contact with the MOF surface whereas the others in the middle of a sufficiently large pore only interact with other xenon atoms as in the bulk liquid. Due to the presence of exchange processes, an averaged chemical shift results. The insert in Figure 3 illustrates this idea. Under the simplifying assumption that the surface is chemically homogeneous and the chemical shift of xenon in surface contact is given by δ_S, one can then write:

$$\bar{\delta} = p_S\delta_S + p_B\delta_B$$
$$p_B = 1 - p_S$$
$$\Delta\delta = \bar{\delta} - \delta_B = p_S(\delta_S - \delta_B) \qquad [2]$$

Here, p_S and p_B denote the probabilities for a xenon atom to be in surface contact or in the bulk liquid, respectively. Thus, $\Delta\delta$ depends on the probability p_S that xenon interacts with the surface. It can be written as:

$$p_S = \frac{N_S}{N_S + N_B}$$

N_S and N_B denote the numbers of xenon atoms in contact with the surface and in the bulk liquid, respectively.

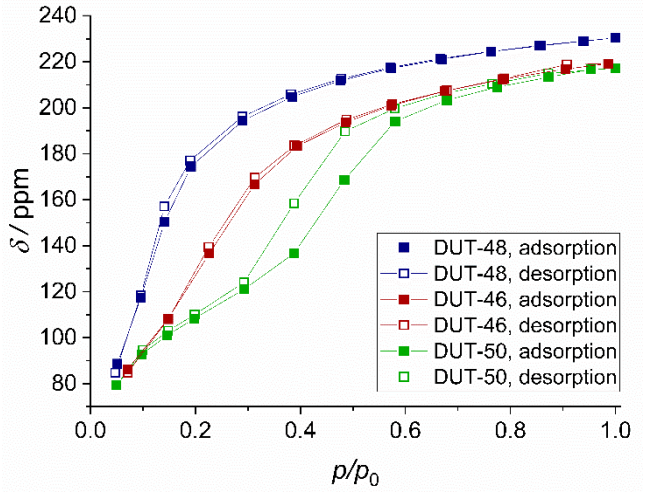

Figure 2. ^{129}Xe NMR adsorption and desorption isotherms of DUT-48, DUT-46, and DUT-50 at 237 K.

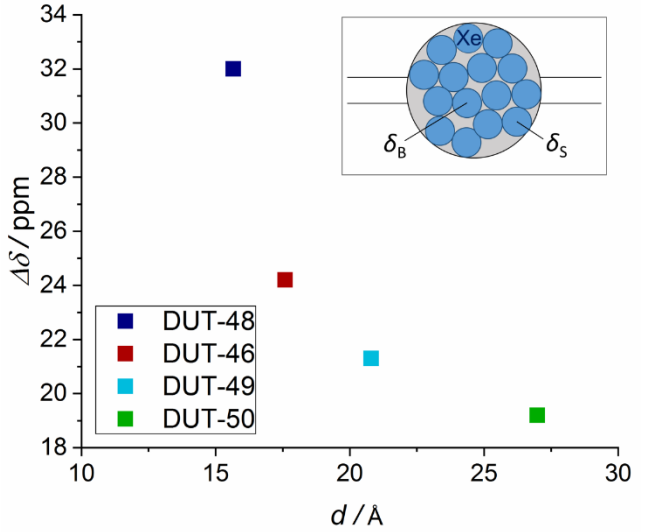

Figure 3. Correlation of the mean pore diameter, d, and the chemical shift difference, $\Delta\delta$, of adsorbed xenon at 237 K for DUT-48, DUT-46, DUT-49, and DUT-50. The insert shows the model of a xenon-filled pore.

The probability for a xenon atom to be in surface contact, however, will depend on the average pore size of the material. In order to test the validity of this consideration, the correlation between $\Delta\delta$ and the average pore diameter of the studied samples (cf. Table 2) is shown in Figure 3. For the materials of the considered isoreticular series, $\Delta\delta$ obviously follows the expected trend: An increasing average pore size leads to decreasing $\Delta\delta$ since the probability for surface contact decreases in larger pores. Assuming spherical pores, one would expect a $1/d$- dependence for p_S. The data do not exactly follow this dependence but show a similar trend. The deviation is not unexpected because the MOFs exhibit not only mesopores but also micropores and the above made assumptions are certainly an oversimplification. In any case, our observations show that $\Delta\delta$ can be used as an easily measurable estimate for the average pore size in MOFs of comparable surface chemistry.

Table 2. Average pore diameter d (for detailed information about the calculation, see Table S2) and chemical shift difference $\Delta\delta$ of adsorbed xenon relative to bulk liquid xenon at 237 K for DUT-48, DUT-46, DUT-49, and DUT-50.

	d / Å	$\Delta\delta$ / ppm
DUT-48	15.66	32.0
DUT-46	17.59	24.2
DUT-49	20.80	21.3
DUT-50	26.98	19.2

Experiments at 200 K. As mentioned above, DUT-49 is rigid at 237 K but becomes flexible at 200 K.[13] The other members of the described isoreticular series were found to be rigid at 237 K as well. In order to characterize the influence of decreasing temperature, their behavior at 200 K

was also studied here. Since the ^{129}Xe chemical shift is very sensitive to structural changes, differences between chemical shift isotherms and the conventional xenon uptake measurements must now be taken into account.

For DUT-48, an almost reversible Type I(b) isotherm is also observed at 200 K (Figure 4). Only a minor hysteresis occurs within the experimental error. That means, the microporous DUT-48 is rigid at both measurement temperatures applied here.

DUT-46 contains both, micropores and small mesopores (see Table 1) and exhibits a type IV adsorption/desorption isotherm. However, the volumetric uptake-derived isotherm does not exhibit a detectable hysteresis. This can be explained by the rather small mesopores (21.8 Å diameter) where capillary condensation not yet plays a major role. However, the NMR-derived ^{129}Xe chemical shift adsorption/desorption isotherm exhibits a considerable hysteresis. It should be noted that the uptake-derived isotherm was measured at an even shorter equilibration time of about 400 s for each data point than the NMR-derived chemical shift isotherm measured with 15 minutes equilibration for each data point. The data in the hysteresis range at relative pressures between 0.1 and 0.3 were even measured after 75 minutes equilibration because the equilibrium is not reached after 15 minutes. This follows from the observation that line width and position still change after 15 minutes (cf. Figure S2). The characteristic difference between the two isotherms, i.e., the absence of a hysteresis in the volumetric uptake-derived data, can thus not be explained by insufficient equilibration time for the NMR experiment. Our explanation for this behavior is a diffusion-limited re-distribution of adsorbed xenon in the pore system. Typically, the small pores fill first at low pressures. However, the windows of the smallest pores have only about 4 Å size and the van-der-Waals diameter of xenon amounts to 4.4 Å. At low pressures, xenon is thus probably not (or only to a limited extent) adsorbed in these small cuboctahedral pores. However, a re-distribution of the adsorbed xenon in the pore system can occur at higher pressure, i.e., the small pores increasingly fill. During desorption, the cuboctahedral pores are still filled and desorption takes place at lower relative pressure. Thus, the hysteresis in the NMR-derived isotherm could be explained. It is already known for another MOF, that xenon is able to pass even smaller pore apertures and is trapped inside afterwards.[36] However, this behavior can be observed at lower temperatures and pressures for DUT-46. In agreement with this idea, the integral intensity of the signal for adsorbed xenon remains almost constant during the whole time of the equilibration experiment of 75 minutes (cf. Figure S3). Only minor changes occur after the first few minutes of equilibration. Thus, the significant change in chemical shift and line shape occurs most likely due to a re-arrangement of already adsorbed xenon atoms. Further work is in progress to clarify this observation. In any case, it can be stated that DUT-46 and DUT-48 do not show the counterintuitive low-temperature NGA behavior of DUT-49. The reason for this is most likely the linker structure. NGA is a spontaneous desorption of gas during pressure increase.[13] Adsorbed xenon is released because the mesopores are contracted. This is accompanied by pronounced deformation (bending) of the linkers. The energy needed for this bending is overcompensated by the higher adsorption enthalpies for guests like methane or xenon.[58] Obviously, the organic linkers used in DUT-48 and DUT-46 are too short and rigid to allow adsorption-driven bending in contrast to DUT-49. However, DUT-50 exhibits an even longer linker than DUT-49 in contrast to DUT-48 and DUT-46. The ^{129}Xe NMR spectra recorded at 200 K are shown in Figure 5 for the adsorption experiment, i.e., steadily increasing pressure along with the volumetric uptake-derived adsorption isotherm. The chemical shift of adsorbed xenon steadily increases from 120 ppm to 150 ppm with relative pressure up to 0.28. At a relative pressure of about 0.3, a sudden shift jump of nearly 100 ppm occurs. This jump is caused by the structural transition from the open-pore (***op***) state to the closed-pore (***cp***) state. The resulting higher probability p_S for xenon to be in contact with the surface in the contracted pores causes the sudden chemical shift in-crease similar like in DUT-49.[31]

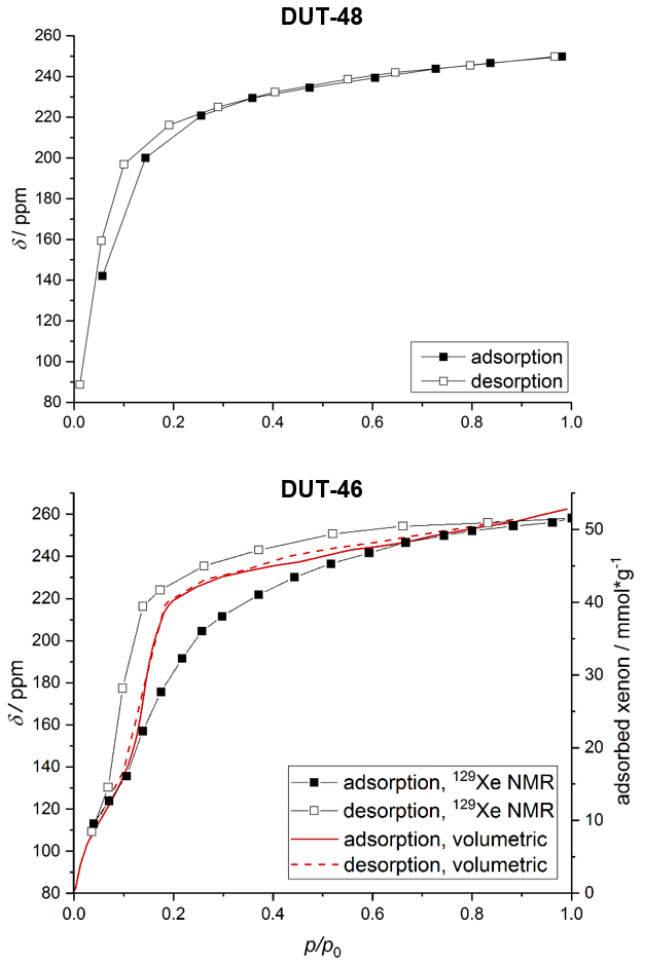

Figure 4. ^{129}Xe NMR adsorption and desorption isotherms of DUT-48 (top) and DUT-46 (bottom) at 200 K.

Further pressure increase results in a moderate increase for the chemical shift of xenon in the ***cp*** state. However, a second signal at a lower chemical shift occurs at relative pressures beyond 0.45. This can be assigned to xenon adsorbed in DUT-50***op***. The transformation of DUT-50 from the ***cp*** state back to the ***op*** state takes place over a relatively wide relative pressure range. At $p/p_0 = 1$, only one signal for xenon remains indicating the complete transformation of DUT-50 into the ***op*** state.

The co-existence of the ***cp*** and ***op*** state over a relatively wide relative pressure range between 0.46 and 0.92 could be explained by two models: (i) the structural transformation is a collective phenomenon of entire crystallites and the sample contains crystallites which exhibit different transition pressures. (ii) the pore opening starts locally at a certain pressure and does then steadily proceed into other regions of the crystallite at increasing pressure (for example, from the surface into the bulk). It is anticipated that the exchange rate of xenon between the ***op*** and ***cp*** state would be slower for the intercrystalline exchange described in (i) than for the intracrystalline exchange in (ii). Therefore, we have measured the exchange rate by 2D EXSY spectroscopy (Figure 6). The exchange rate can be calculated from the dependence of the intensity ratio between cross peaks and diagonal peaks on the mixing time τ_m. For a two-site exchange, the ratio between the intensities of cross peaks, I_{cross}, and diagonal peaks, $I_{diagonal}$, is described by the function[59]

$$\frac{I_{cross}}{I_{diagonal}} \sim \tanh(k_{ex}\tau_m) \qquad [3]$$

Figure 6 demonstrates that the data indeed follow this function. An exchange rate k_{ex} of 95 Hz could be measured corresponding to a characteristic exchange time constant of 11 ms. This is a typical value for intercrystalline exchange processes in microcrystalline materials.[51,60] It is thus anticipated that the ***op***-***cp*** structural transition in DUT-50 is a collective switching of entire crystallites in an ensemble of crystallites with slightly varying switching pressure and not a local phenomenon continuously spreading out within one crystallite. During desorption experiment (see Figure 7), the structural change from DUT-50***op*** to DUT-50***cp*** occurs at p/p_0 = 0.3. The material stays in this state even at very low pressure down to 0.01. That means, the described structural transitions are not reversible.

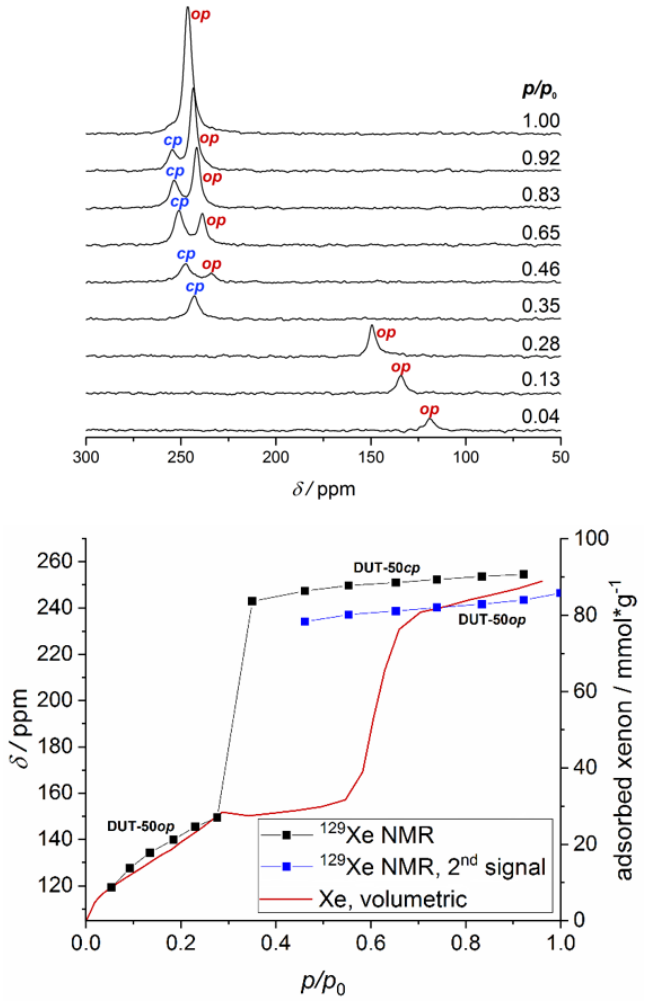

Figure 5. ^{129}Xe NMR adsorption spectra (top) and ^{129}Xe NMR and volumetric uptake-derived xenon adsorption isotherms (bottom) of DUT-50 at 200 K.

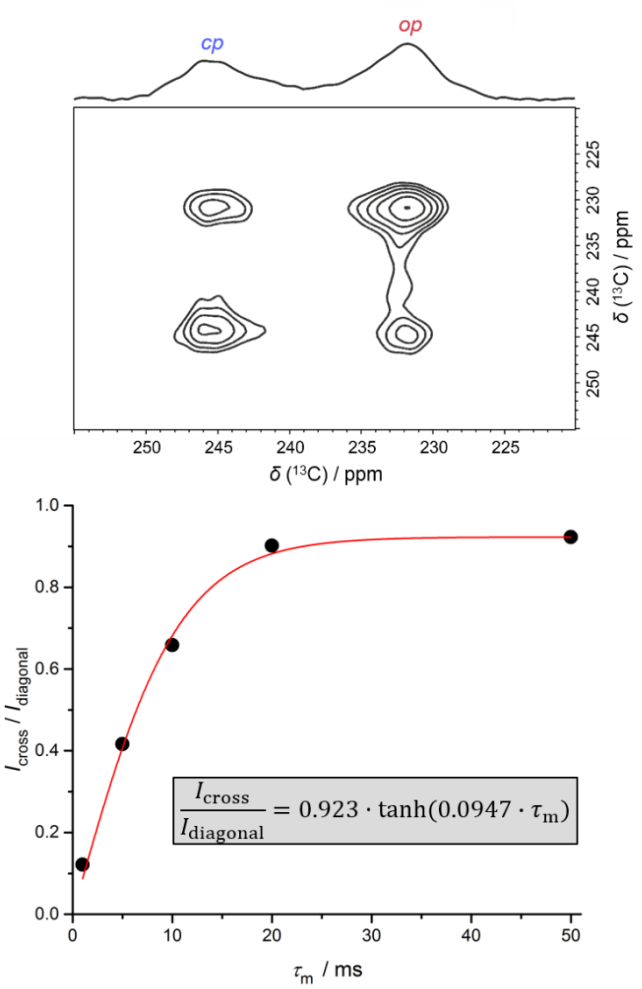

Figure 6. EXSY spectra of xenon adsorbed on DUT-50 at p = 2.0 bar and 200 K (top) and correlation between the mixing time and the intensity ratio of cross peaks and diagonal peaks measured as a function of the mixing time. The red line was determined by fitting the data to eq. [3].

The adsorption/desorption isotherm obtained from the ^{129}Xe NMR spectra can be compared with the volumetric xenon isotherms (cf. Figures 5 and 7, bottom). During adsorption, the jump of the chemical shift takes place coinciding with the NGA transition. The appearance of the second signal for adsorbed xenon shows the gradual transformation of the ***cp*** state back to the ***op*** state. During desorption the structural change of DUT-50 is only observable within the ^{129}Xe NMR isotherm, rendering ^{129}Xe NMR spectroscopy highly useful to better understand the structural transformation. It can thus be stated that DUT-50 is the second known material showing the negative gas adsorption phenomenon.

Finally, another MOF denoted as DUT-151 (cf. Figure S4) with an even longer linker than DUT-50 (four 1,4 substituted phenylene units in the ligand backbone) was also investigated with respect to its xenon adsorption behavior. Due to its interpenetrated network structure, the MOF was not included into the pore size estimation experiments.

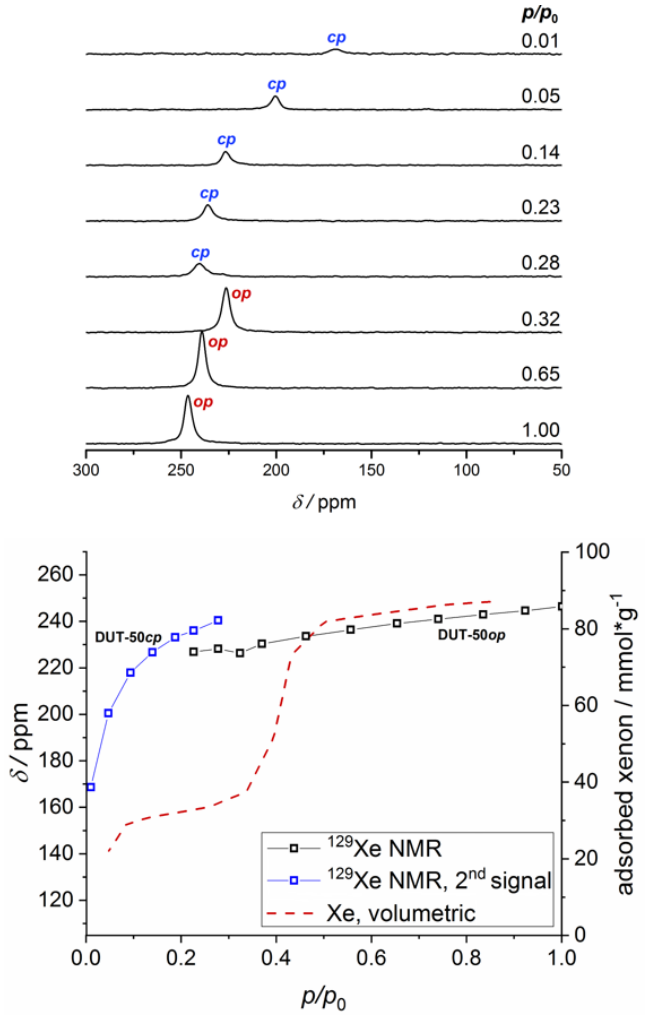

Figure 7. ^{129}Xe NMR desorption spectra (top) and ^{129}Xe NMR and volumetric uptake-derived xenon desorption isotherms (bottom) of DUT-50 at 200 K.

Nevertheless, the adsorption experiments at 200 K were performed for DUT-151 as well. The material shows structural transformations during adsorption at this temperature which, however, differ from the behavior of DUT-50. After activation (DUT-151***act***) and start of the adsorption experiment at low pressure, the material is found in the closed-pore state (DUT-151***cp***). At low pressure, the signal of adsorbed xenon is observed in the range between 118 ppm and 158 ppm (Figure 8). This signal can be assigned to xenon adsorbed on the closed pores at low pressures. Beyond a relative pressure of 0.2, a second signal for adsorbed xenon occurs at a higher chemical shift of 202 ppm. Thus, two signals can be observed simultaneously in this pressure range. However, the signal intensity of the first signal at lower chemical shift decreases with increasing pressure and the signal finally disappears.

We assume, that the interpenetrated networks shift relative to each other beginning from a relative pressure of 0.2, i.e., the network seems to transform from the closed-pore structure to an open-pore structure (DUT-151***op***). The chemical shift jump and the appearance of the second signal is clearly visible within the adsorption isotherm of

DUT-151 at 200 K (Figure 8, bottom). This pore opening allows more

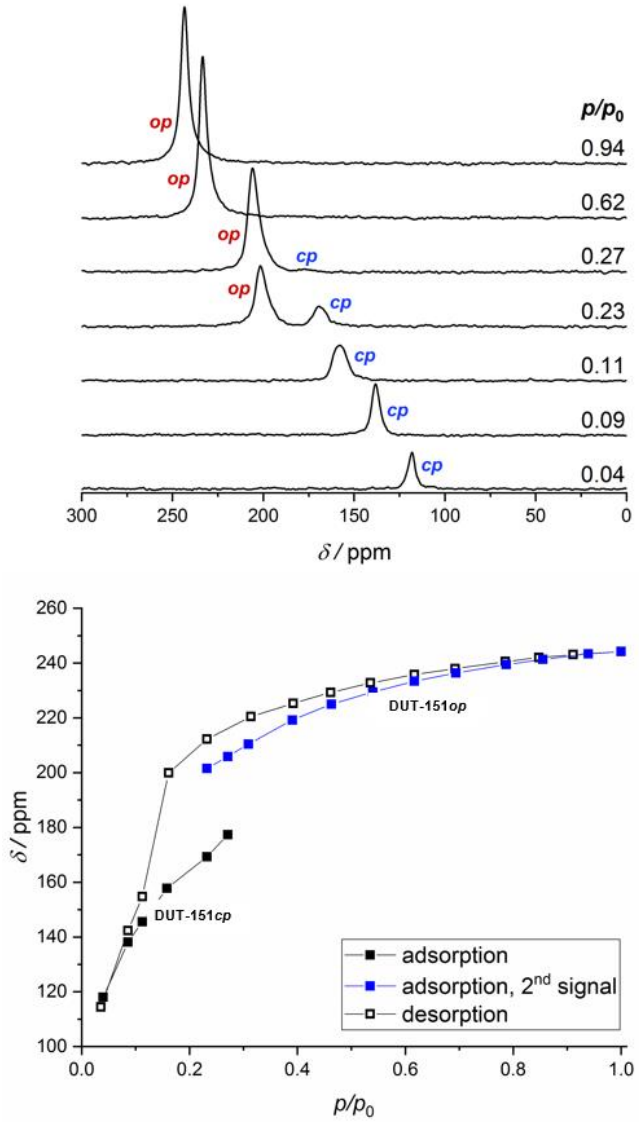

Figure 8. ^{129}Xe NMR adsorption spectra (top) and ^{129}Xe NMR adsorption and desorption isotherm (bottom) of DUT-151 at 200 K.

xenon adsorption as seen from the increasing total signal intensity. The tendency of the lattice to close – which must be overcome by adsorbed xenon – as well as Xe-Xe interactions may cause the higher chemical shift of the second signal. During desorption, only one signal of adsorbed xenon is recorded and a hysteresis is observed. The chemical shift jump is observable during desorption at lower relative pressure of 0.15. The starting value of the chemical shift of adsorbed xenon is reached again after desorption of gas and thus, the adsorption-induced structural transition seems to be reversible. The reason for the difference in adsorption and switching behavior compared with DUT-49 and DUT-50 (see above) is the lattice interpenetration present in DUT-151. This was found to prevent large scale structural contraction and NGA due to a reduced void. However, sufficient void space in the pores is required for such a structural transition.

CONCLUSSION

High pressure *in situ* ^{129}Xe NMR spectroscopy is well-suited to investigate host-guest interactions and adsorption processes in porous materials such as MOFs. The following conclusions are drawn from our studies:

(1) Chemical shift measurement of adsorbed xenon as a function of pressure yields chemical shift adsorption/desorption isotherms which compare well with conventional, uptake-measurement based isotherms for rigid MOFs. This is due to the fact that the chemical shift and the density of adsorbed xenon are correlated.

(2) The difference $\Delta\delta$ between the chemical shift of adsorbed xenon extrapolated to a relative pressure of one and the chemical shift of bulk liquid xenon correlates with the average pore diameter for MOFs of comparable chemical composition, i.e., surface chemistry. This correlation between $\Delta\delta$ and the mean pore diameter is demonstrated for the series of isoreticular MOFs studied here (DUT-48, DUT-46, DUT-49, and DUT-50). The chemical shift difference of adsorbed xenon decreases with increasing mean pore diameter. The quantity $\Delta\delta$ is easily and accurately measurable by high-pressure *in situ* ^{129}Xe NMR spectroscopy and allows an estimation of the mean pore size.

(3) Characterization of the adsorption processes at lower temperature (200 K) shows interesting adsorption phenomena. Similar to DUT-49, the novel compound DUT-50 also shows structural changes of the pore system during adsorption causing negative gas adsorption (NGA) as can be visualized by ^{129}Xe NMR spectroscopy. 2D EXSY experiments allow to measure the exchange between coexisting open and contracted pores. The measured exchange rate suggests that structural transitions in DUT-50 are a rather collective phenomenon of entire crystallites.

(4) The interpenetrated compound DUT-151 shows a different switching behavior compared with DUT-49 and DUT-50. The transition is not a structural contraction but a xenon-adsorption induced mutual shift of the two interpenetrating networks from a closed-pore to an open-pore state of the MOF.

(5) The non-flexible compound DUT-46 exhibits a hysteresis in the ^{129}Xe NMR isotherm due to diffusion-limited adsorption/re-distribution processes at low temperature.

ASSOCIATED CONTENT

Supporting Information

MOF synthesis and calculation of the pore sizes of the different materials, additional ^{129}Xe NMR spectra and the structure of DUT-151.

AUTHOR INFORMATION

Corresponding Author

*Prof. Dr. Eike Brunner
eike.brunner@tu-dresden.de

Funding Sources

Financial support from the DFG (FOR2433: MOF Switches) is gratefully acknowledged. Moreover, this project has received funding from the European Research Council (ERC) under the European Union's Horizon 2020 research and innovation programme (grant agreement No. 742743). The authors thank the BMBF (No. 05K16OD1) and ANR/DFG Program FUN for financial support.

REFERENCES

(1) Furukawa, H.; Cordova, K. E.; O'Keeffe, M.; Yaghi, O. M. The Chemistry and Applications of Metal-Organic Frameworks. *Science* **2013**, *341*, 974.

(2) Kitagawa, S.; Kitaura, R.; Noro, S. Functional Porous Coordination Polymers. *Angew. Chemie - Int. Ed.* **2004**, *43*, 2334–2375.

(3) Eddaoudi, M.; Kim, J.; Rosi, N.; Vodak, D.; Wachter, J.; O'Keeffe, M.; Yaghi, O. M. Systematic Design of Pore Size and Functionality in Isoreticular MOFs and Their Application in Methane Storage. *Science* **2002**, *295*, 469–472.

(4) Pettinari, C.; Marchetti, F.; Mosca, N.; Tosi, G.; Drozdov, A. Application of Metal – Organic Frameworks. *Polym. Int.* **2017**, *66*, 731–744.

(5) Li, P.; Vermeulen, N. A.; Malliakas, C. D.; Gómez-Gualdrón, D. A.; Howarth, A. J.; Mehdi, B. L.; Dohnalkova, A.; Browning, N. D.; O'Keeffe, M.; Farha, O. K. Bottom-up Construction of a Superstructure in a Porous Uranium-Organic Crystal. *Science* **2017**, *356*, 624–627.

(6) Raschke, S.; Evans, J. D.; Senkovska, I.; Bon, V.; Baburin, I. A.; Kaskel, S.; Bönisch, N.; Hönicke, I. M. Balancing Mechanical Stability and Ultrahigh Porosity in Crystalline Framework Materials. *Angew. Chem. Int. Ed.* **2018**, *57*, 13780–13783.

(7) Schneemann, A.; Bon, V.; Schwedler, I.; Senkovska, I.; Kaskel, S.; Fischer, R. A. Flexible Metal–organic Frameworks. *Chem. Soc. Rev.* **2014**, *43*, 6062–6096.

(8) Stassen, I.; Burtch, N.; Talin, A.; Falcaro, P.; Allendorf, M.; Ameloot, R. An Updated Roadmap for the Integration of Metal–organic Frameworks with Electronic Devices and Chemical Sensors. *Chem. Soc. Rev.* **2017**, *46*, 3185–3241.

(9) Hendon, C. H.; Rieth, A. J.; Korzyński, M. D.; Dincă, M. Grand Challenges and Future Opportunities for Metal-Organic Frameworks. *ACS Cent. Sci.* **2017**, *3*, 554–563.

(10) Horcajada, P.; Serre, C.; Maurin, G.; Ramsahye, N. A.; Balas, F.; Sebban, M.; Taulelle, F. Flexible Porous Metal-Organic Frameworks for a Controlled Drug Delivery. *J. Am. Chem. Soc.* **2008**, *130*, 6774–6780.

(11) Park, H. J.; Suh, M. P. Stepwise and Hysteretic Sorption of N_2, O_2, CO , and H_2 Gases in a Porous Metal – Organic Framework $[Zn_2(BPnDC)_2(bpy)]$. *Chem. Commun.* **2010**, *46*, 610–612.

(12) Klein, N.; Herzog, C.; Sabo, M.; Senkovska, I.; Paasch, S.; Lohe, M. R. Monitoring Adsorption-Induced Switching by ^{129}Xe NMR Spectroscopy in a New Metal – Organic Framework $Ni_2(2,6\text{-ndc})_2(dabco)$. *Phys. Chem. Chem. Phys.* **2010**, *12*, 11778–11784.

(13) Krause, S.; Bon, V.; Senkovska, I.; Stoeck, U.; Wallacher, D.; Többens, D. M.; Zander, S.; Pillai, R. S.; Maurin, G.; Coudert, F.-X.; Kaskel, S. A Pressure-Amplifying Framework Material with Negative Gas Adsorption Transitions. *Nature* **2016**, *532*, 348–352.

(14) Férey, G.; Serre, C. Large Breathing Effects in Three-Dimensional Porous Hybrid Matter: Facts, Analyses, Rules and Consequences. *Chem. Soc. Rev.* **2009**, *38*, 1380–1399.

(15) Sutrisno, A.; Huang, Y. Solid-State NMR: A Powerful Tool for Characterization of Metal-Organic Frameworks. *Solid State Nucl. Magn. Reson.* **2013**, *49-50*, 1–11.

(16) Hoffmann, H. C.; Debowski, M.; Müller, P.; Paasch, S.; Senkovska, I.; Kaskel, S.; Brunner, E. Solid-State NMR Spectroscopy of Metal-Organic Framework Compounds (MOFs). *Materials (Basel).* **2012**, *5*, 2537–2572.

(17) Bon, V.; Pallmann, J.; Eisbein, E.; Hoffmann, H. C.; Senkovska, I.; Schwedler, I.; Schneemann, A.; Henke, S.; Wallacher, D.; Fischer, R. A.; Seifert, G.; Brunner, E.; Kaskel, S. Characteristics of Flexibility in Metal-Organic Framework Solid Solutions of Composition $[Zn_2(BME\text{-}bdc)_x(DB\text{-}bdc)_{2-x}dabco]_n$: In Situ Powder X-Ray Diffraction, in Situ NMR Spectroscopy, and Molecular Dynamics Simulations. *Microporous Mesoporous Mater.* **2015**, *216*, 64–74.

(18) Sin, M.; Kutzscher, C.; Senkovska, I.; Ben, T.; Qiu, S.; Kaskel, S.; Brunner, E. Surface Polarity Estimation of Metal–Organic Frameworks Using Liquid-Phase Mixture Adsorption. *Microporous Mesoporous Mater.* **2017**, *251*, 129–134.

(19) Kemnitzer, T. W.; Tschense, C. B. L.; Wittmann, T.; Rössler, E. A.; Senker, J. Exploring Local Disorder within CAU-1 Frameworks Using Hyperpolarized ^{129}Xe NMR Spectroscopy. *Langmuir* **2018**, *34*, 12538–12548.

(20) Gul-E-Noor, F.; Mendt, M.; Michel, D.; Pöppl, A.; Krautscheid, H.; Haase, J.; Bertmer, M. Adsorption of Small Molecules on $Cu_3(btc)_2$ and $Cu_{3-x}Zn_x(btc)_2$ Metal-Organic Frameworks (MOF) as Studied by Solid-State NMR. *J. Phys. Chem. C* **2013**, *117*, 7703–7712.

(21) Milner, P. J.; Siegelman, R. L.; Forse, A. C.; Gonzalez, M. I.; Runčevski, T.; Martell, J. D.; Reimer, J. A.; Long, J. R. A Diaminopropane-Appended Metal-Organic Framework Enabling Efficient CO_2 Capture from Coal Flue Gas via a Mixed Adsorption Mechanism. *J. Am. Chem. Soc.* **2017**, *139*, 13541–13553.

(22) Kong, X.; Scott, E.; Ding, W.; Mason, J. A.; Long, J. R.; Reimer, J. A. CO_2 Dynamics in a Metal-Organic Framework with Open Metal Sites. *J. Am. Chem. Soc.* **2012**, *134*, 14341–14344.

(23) Witherspoon, V. J.; Xu, J.; Reimer, J. A. Solid-State NMR Investigations of Carbon Dioxide Gas in Metal-Organic Frameworks: Insights into Molecular Motion and Adsorptive Behavior. *Chem. Rev.* **2018**, *118*, 10033–10048.

(24) Wong, Y. T. A.; Martins, V.; Lucier, B. E. G.; Huang, Y. Solid-State NMR Spectroscopy: A Powerful Technique to Directly Study Small Gas Molecules Adsorbed in Metal–Organic Frameworks. *Chem. - A Eur. J.* **2019**, *25*, 1848–1853.

(25) Bassanetti, I.; Bracco, S.; Comotti, A.; Negroni, M.; Bezuidenhout, C.; Canossa, S.; Mazzeo, P. P.; Marchió, L.; Sozzani, P. Flexible Porous Molecular Materials Responsive to CO_2, CH_4 and Xe Stimuli. *J. Mater. Chem. A* **2018**, *6*, 14231–14239.

(26) Bonardet, J.-L. L.; Fraissard, J.; Gedeon, A.; Springuel-Huet, M.-A. A. Nuclear Magnetic Resonance of Physisorbed Xe-129 Used as a Probe to Investigate Porous Solids. *Catal. Rev. Eng.* **1999**, *41*, 115–225.

(27) Weiland, E.; Springuel-Huet, M. A.; Nossov, A.; Gédéon, A. ^{129}Xenon NMR: Review of Recent Insights into Porous Materials. *Microporous Mesoporous Mater.* **2016**, *225*, 41–65.

(28) Ito, T.; Fraissard, J. ^{129}Xe NMR Study of Xenon Adsorbed on Y Zeolites. *J. Chem. Phys.* **1982**, *76*, 5225–5229.

(29) Demarquay, J.; Fraissard, J. ^{129}Xe NMR of Xenon Adsorbed on Zeolites. Relationship between the Chemical Shift and the Void Space. *Chem. Phys. Lett.* **1987**, *136*, 314–318.

(30) Meersmann, T.; Brunner, E. *Hyperpolarized Xe-129 Magnetic Resonance*; The Royal Society of Chemistry: Cambridge, Great Britain, 2015.

(31) Schaber, J.; Krause, S.; Paasch, S.; Senkovska, I.; Bon, V.; Többens, D. M.; Wallacher, D.; Kaskel, S.; Brunner, E. In Situ Monitoring of Unique Switching Transitions in the Pressure-Amplifying Flexible Framework Material DUT-49 by High-

Pressure ^{129}Xe NMR Spectroscopy. *J. Phys. Chem. C* **2017**, *121*, 5195–5200.
(32) Chmelka, B. F.; Raftery, D.; McCormick, A. V.; De Menorval, L. C.; Levine, R. D.; Pines, A. Measurement of Xenon Distribution Statistics in Na-A Zeolite Cavities. *Phys. Rev. Lett.* **1991**, *66*, 580–583.
(33) Jameson, A. K.; Jameson, C. J.; Gerald, R. E. Cage-to-Cage Migration Rates of Xe Atoms in Zeolite NaA from Magnetization Transfer Experiments and Simulations. *J. Chem. Phys.* **1994**, *101*, 1775–1786.
(34) Jameson, A. K.; Jameson, C. J.; de Dios, A. C.; Oldfield, E.; Gerald, R. E.; Turner, G. L. ^{129}Xe Magic-Angle Spinning Spectra of Xenon in Zeolite NaA Direct Observation of Distributions of Mixed Clusters of Coadsorbed Species. *Solid State Nucl. Magn. Reson.* **1995**, *4*, 1–12.
(35) Moudrakovski, I. L.; Ratcliffe, C. I.; Ripmeester, J. a. ^{129}Xe NMR Study of Adsorption and Dynamics of Xenon in AgA Zeolite. *J. Am. Chem. Soc.* **1998**, *120*, 3123–3132.
(36) Bunzen, H.; Kolbe, F.; Kalytta-Mewes, A.; Sastre, G.; Brunner, E.; Volkmer, D. Achieving Large Volumetric Gas Storage Capacity in Metal-Organic Frameworks by Kinetic Trapping: A Case Study of Xenon Loading in MFU-4. *J. Am. Chem. Soc.* **2018**, *140*, 10191–10197.
(37) Springuel-Huet, M. A.; Fraissard, J. ^{129}Xe NMR of Xenon on the Molecular Sieves $AlPO_4$–11 and SAPO-11. Chemical Shift Anisotropy Related to the Asymmetry of the Adsorption Zones. *Chem. Phys. Lett.* **1989**, *154*, 299–302.
(38) Moudrakovski, I.; Soldatov, D. V; Ripmeester, J. a; Sears, D. N.; Jameson, C. J. Xe NMR Lineshapes in Channels of Peptide Molecular Crystals. *Proc. Natl. Acad. Sci. U. S. A.* **2004**, *101*, 17924–17929.
(39) Soldatov, D. V; Moudrakovski, I. L.; Grachev, E. V; Ripmeester, J. A. Micropores in Crystalline Dipeptides as Seen from the Crystal Structure, He Pycnometry, and ^{129}Xe NMR Spectroscopy. *J. Am. Chem. Soc.* **2006**, *128*, 6737–6744.
(40) Brouwer, D. H.; Moudrakovski, I. L.; Udachin, K. A.; Enright, G. D.; Ripmeester, J. A. Guest Loading and Multiple Phases in Single Crystals of the van Der Waals Host P-Tert-butylcalix[4]arene. *Cryst. Growth Des.* **2008**, *8*, 1878–1885.
(41) Jameson, C. J.; Jameson, A. K.; Gerald, R. E.; Lim, H.-M. Anisotropic Xe Chemical Shifts in Zeolites. The Role of Intra- and Intercrystallite Diffusion. *J. Phys. Chem. B* **1997**, *101*, 8418–8437.
(42) Springuel-Huet, M. A.; Nossov, A.; Adem, Z.; Guenneau, F.; Volkringer, C.; Loiseau, T.; Férey, G.; Gédéon, A. ^{129}Xe NMR Study of the Framework Flexibility of the Porous Hybrid MIL-53(Al). *J. Am. Chem. Soc.* **2010**, *132*, 11599–11607.
(43) Böhlmann, W.; Pöppl, A.; Sabo, M.; Kaskel, S. Characterization of the Metal–Organic Framework Compound Cu_3(benzene 1,3,5-tricarboxylate)$_2$ by Means of ^{129}Xe Nuclear Magnetic and Electron Paramagnetic Resonance Spectroscopy. *J. Phys. Chem. B* **2006**, *110*, 20177–20181.
(44) Ueda, T.; Kurokawa, K.; Eguchi, T.; Kachi-Terajima, C.; Takamizawa, S. Local Structure and Xenon Adsorption Behavior of Metal-Organic Framework System $[M_2(O_2CPh)_4(pyz)]_n$ (M = Rh and Cu) as Studied with Use of Single-Crystal X-Ray Diffraction, Adsorption Isotherm, and Xenon-129 NMR. *J. Phys. Chem. C* **2007**, *111*, 1524–1534.
(45) Ooms, K. J.; Wasylishen, R. E. ^{129}Xe NMR Study of Xenon in Iso-Reticular Metal-Organic Frameworks. *Microporous Mesoporous Mater.* **2007**, *103*, 341–351.
(46) Raftery, D.; Long, H.; Meersmann, T.; Grandinetti, P. J.; Reven, L.; Pines, A. High-Field NMR of Adsorbed Xenon Polarized by Laser Pumping. *Phys. Rev. Lett.* **1991**, *66*, 584–587.
(47) Sozzani, P.; Comotti, A.; Simonutti, R.; Meersmann, T.; Logan, J. W. A Porous Crytalline Molecular Solid Explored by Hyperpolarized Xenon. *Angew. Chem. Int. Ed.* **2000**, *39*, 2695–2699.
(48) Cheng, C. Y.; Bowers, C. R. Direct Observation of Atoms Entering and Exiting L-Alanyl-L-Valine Nanotubes by Hyperpolarized Xenon-129 NMR. *J. Am. Chem. Soc.* **2007**, *129*, 13997–14002.
(49) Comotti, A.; Bracco, S.; Valsesia, P.; Ferretti, L.; Sozzani, P. 2D Multinuclear NMR, Hyperpolarized Xenon and Gas Storage in Organosilica Nanochannels with Crystalline Order in the Walls. *J. Am. Chem. Soc.* **2007**, *129*, 8566–8576.
(50) Cheng, C. Y.; Stamatatos, T. C.; Christou, G.; Bowers, C. R. Molecular Wheels as Nanoporous Materials: Differing Modes of Gas Diffusion through Ga_{10} and Ga_{18} Wheels Probed by Hyperpolarized ^{129}Xe NMR Spectroscopy. *J. Am. Chem. Soc.* **2010**, *132*, 5387–5393.
(51) Hoffmann, H. C.; Assfour, B.; Epperlein, F.; Klein, N.; Paasch, S.; Senkovska, I.; Kaskel, S.; Seifert, G.; Brunner, E. High-Pressure in Situ ^{129}Xe NMR Spectroscopy and Computer Simulations of Breathing Transitions in the Metal–Organic Framework Ni_2(2,6-Ndc)$_2$(dabco) (DUT-8(Ni)). *J. Am. Chem. Soc.* **2011**, *133*, 8681–8690.
(52) Stoeck, U.; Krause, S.; Bon, V.; Senkovska, I.; Kaskel, S. A Highly Porous Metal–organic Framework, Constructed from a Cuboctahedral Super-Molecular Building Block, with Exceptionally High Methane Uptake. *Chem. Commun.* **2012**, *48*, 10841–10843.
(53) Raiford, D. S.; Fisk, C. L.; Becker, E. D. Calibration of Methanol and Ethylene Glycol Nuclear Magnetic Resonance Thermometers. *Anal. Chem.* **1979**, *51*, 2050–2051.
(54) Van Geet, A. L. Calibration of Methanol Nuclear Magnetic Resonance Thermometer at Low Temperature. *Anal. Chem.* **1970**, *42*, 679–680.
(55) Thommes, M.; Kaneko, K.; Neimark, A. V.; Olivier, J. P.; Rodriguez-Reinoso, F.; Rouquerol, J.; Sing, K. S. W. Physisorption of Gases, with Special Reference to the Evaluation of Surface Area and Pore Size Distribution (IUPAC Technical Report). *Pure Appl. Chem.* **2015**, *87*, 1051–1069.
(56) Trepte, K.; Schaber, J.; Schwalbe, S.; Drache, F.; Senkovska, I.; Kaskel, S.; Kortus, J.; Brunner, E.; Seifert, G. The Origin of the Measured Chemical Shift of ^{129}Xe in UiO-66 and UiO-67 Revealed by DFT Investigations. *Phys. Chem. Chem. Phys.* **2017**, *19*, 10020–10027.
(57) Cavka, J. H.; Olsbye, U.; Guillou, N.; Bordiga, S.; Lillerud, K. P. A New Zirconium Inorganic Building Brick Forming Metal Organic Frameworks with Exceptional Stability. *J. Am. Chem. Soc.* **2008**, *6*, 1–19.
(58) Evans, J. D.; Bocquet, L.; Coudert, F.-X. Origins of Negative Gas Adsorption. *Chem* **2016**, *1*, 873–886.
(59) Levitt, M. H. *Spin Dynamics: Basics of Nuclear Magnetic Resonance*, 2. Auflage.; John Wiley & Sons Ltd: Chichester, Great Britain, 2008.
(60) Giovine, R.; Volkringer, C.; Springuel-Huet, M. A.; Nossov, A.; Blanc, F.; Trébosc, J.; Loiseau, T.; Amoureux, J. P.; Lafon, O.; Pourpoint, F. Study of Xenon Mobility in the Two Forms of MIL-53(Al) Using Solid-State NMR Spectroscopy. *J. Phys. Chem. C* **2017**, *121*, 19262–19268.

High pressure *in situ* ^{129}Xe NMR spectroscopy is used to investigate host-guest interactions and adsorption processes in novel MOFs isoreticular to the flexible DUT-49 at different temperatures. A correlation between the chemical shift of adsorbed xenon and the mean pore diameter is demonstrated for DUT-48, DUT-46, DUT-49, and DUT-50.